02,13

Influence of transmission line parameters on the degree of matching of the generator with the SIS-mixer in the frequency range 200−700 GHz

© A.A. Atepalikhin[1,2,3], F.V. Khan[1,2,3], L.V. Filippenko[1], V.P. Koshelets[1,2]

[1] Kotelnikov Institute of Radio Engineering and Electronics, Russian Academy of Sciences, Moscow, Russia
[2] Institute of Physics of Microstructures, Russian Academy of Sciences, Nizhny Novgorod, Russia
[3] Moscow Institute of Physics and Technology (State University), Dolgoprudnyi, Moscow oblast, Russia

E-mail: atepalikhin@hitech.cplire.ru

Received April 29, 2022
Revised April 29, 2022
Accepted May 12, 2022

This work is aimed at the development, research and optimization of superconducting integrated circuits designed to match the impedances of a long Josephson junction generator, the so-called flux generator (FFO) and a superconductor–insulator–superconductor (SIS) detector in the sub-terahertz frequency range. Numerical calculations of integrated circuits designed to optimize the parameters of transmission lines are presented. The main parameters of the lines and their influence on signal propagation are determined. The results of optimization of integrated matching circuits in the range of 450−700 GHz are demonstrated.

Keywords: integrated matching circuits, Josephson junctions, sub-terahertz generator.

DOI: 10.21883/PSS.2022.10.54219.41HH

1. Introduction

The development of technologies for generating and recording radiation in the terahertz frequency range is relevant not only for scientific research in various territories of physics, astronomy, metrology and biology, but also for a number of applied problems, for example, in medicine and security systems. The shortfall of solid-state sources of continuous terahertz radiation with the possibility of smooth frequency tuning, which is especially pronounced in the frequency range from 500 GHz to 1.5 THz, motivates works on their development and research. Improvement of integral matching structures (microwave signal transmission lines) will make it possible to create and study sources of terahertz radiation based on an array of synchronously operating transitions that provide frequency tuning in a wide frequency range. In addition, similar circuits will be used in the design of a new generation of integrated receivers in the sub-terahertz range [1,2].

The niobium integrated structures under study are designed to operate in the range of 200−700 GHz. The process of their modernization consists in optimizing the design of the constituent elements and selecting the parameters of the transmission line, such as the thickness and material of the dielectric layer, the geometric dimensions of the structural elements, detector characteristics and temperature. Structure optimization is carried out at the design stage of the device using existing models that take into account the penetration of a magnetic field into superconductor, as well as losses in niobium electrodes at voltages of the order of and above the gap voltage [3]. The core target of the work is the creation and testing of numerical calculation methods that make it possible to correctly describe experimental superconducting structures in a wide frequency range from 200 to 700 GHz, as well as to optimize matching structures in the desired frequency range. For optimization, it is essential to determine the influence of the above factors on the matching factor and its dependence on frequency. This work is devoted to the solution of these issues.

2. Integral matching structures and methods of their study

The microwave radiation generator is a distributed Josephson junction (DJJ) [1,4–6], in the English literature known as the flux-flow oscillator (FFO), which operates in the sub-terahertz frequency range from 200 to 700 GHz [2,7,8]. A lumped Josephson junction superconductor-insulator-superconductor (SIS) is used as a high-frequency signal detector. Both devices are located on the same substrate, the radiation propagates from the flux-flow oscillator (FFO) to the SIS along special transmission line shown in Fig. 1.

The role of each several components is essential; the elements of the transmission line are selected in such a way as to ensure the maximum matching of the impedances of the generator and the detector in the widest possible frequency band [8]. To ensure independent power supply of the generator *1* and the detector *5*, DC decoupling of these elements *3* is required, which should not interfere with the

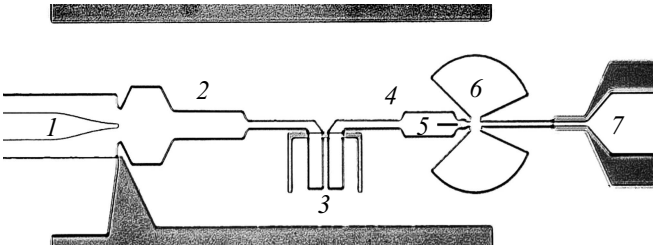

Figure 1. Photo of the integral matching structure. *1* is FFO, *2* is three-stage impedance transformer, *3* is low-frequency break element, *4* is two-stage impedance transformer, *5* is SIS detector, *6* is radial contactor, *7* is output coplanar line.

passage of the high-frequency signal from the generator to the detector. To do this, the schema provides a DC break, made in the form of a slot antenna. The SIS detector *5* has a large parasitic capacitance, which can be „detuned“ at the operating frequency by connecting the small inductance made in the form of a segment of microstrip line a few micrometers long. To connect the inductance to ground by high frequency, „a blocking“ capacitor is used, which is implemented using broadband radial contactors *6*. It should be noted that the output impedance of the generator is a fraction of an ohm, which makes it necessary to use a multi-sectional impedance transformer *2* to match the decoupling circuit and to connect to the detector.

In the work, the results of the study of integrated circuits prepared on the basis of Nb−AlO_x−Nb and Nb−AlN−NbN tunnel structures are presented. The technology for manufacturing superconducting integrated structures based on high-quality tunnel junctions was developed and optimized at the Kotelnikov Institute of Radio Engineering and Electronics of RAS [9,10]; this technology has been tested in the manufacture of low-noise THz receiver devices for radio astronomy and integrated receivers for atmospheric monitoring and laboratory applications [2,7,11,12]. The main elements of matching circuits are made in the form of segments of microstrip lines based on niobium films; a layer of silicon dioxide SiO_2 was used as insulator. Two variants were studied with a variation in the thickness of SiO_2 in the matching structure. In the first variant, the SiO_2 thickness was 400 nm over the entire scheme, except for the first section of the transformer *2*, where the layer thickness was 200 nm, to reduce the wave resistance of the adjacent to FFO line. In the second variant, an insulator layer of the same SiO_2 thickness was used throughout the circuit, equal to 250 nm, which simplifies the technology for manufacturing integrated structures, but can narrow the matching band and worsen signal transmission.

Experimental determination of the degree of matching for the impedances of the generator and the detector is carried out by measuring the dependence of the power absorbed in the detector on the generator radiation frequency. The power released in the transition can be estimated by comparing experimental data with calculations within the Tucker and Feldman theory [13]. Absorbed power magnitude is proportional to the square of the pumping current I_{pump} of the SIS detector at voltage under the slot, where a quasiparticle step is formed due to electron tunneling under the action of a high-frequency signal; the value of the current at this stage is measured in the experiment (see Fig. 2, *a*). The main parameters of the above SIS junction are: $R_nS = 27.2\,\Omega\cdot\mu\text{m}^2$, $S = 1.14\,\mu\text{m}^2$, where R_n is normal junction resistance, S is junction area. To compare different circuits, the pumping current is normalized to a certain maximum value; usually, for normalization, the magnitude of the value of current step on the slot I_g is used. The frequency of microwave radiation is determined by the voltage on the FFO according to the Josephson relation. The signal power at a given frequency is proportional to the FFO current and can be varied by simultaneously adjusting the magnetic field and current of the FFO.

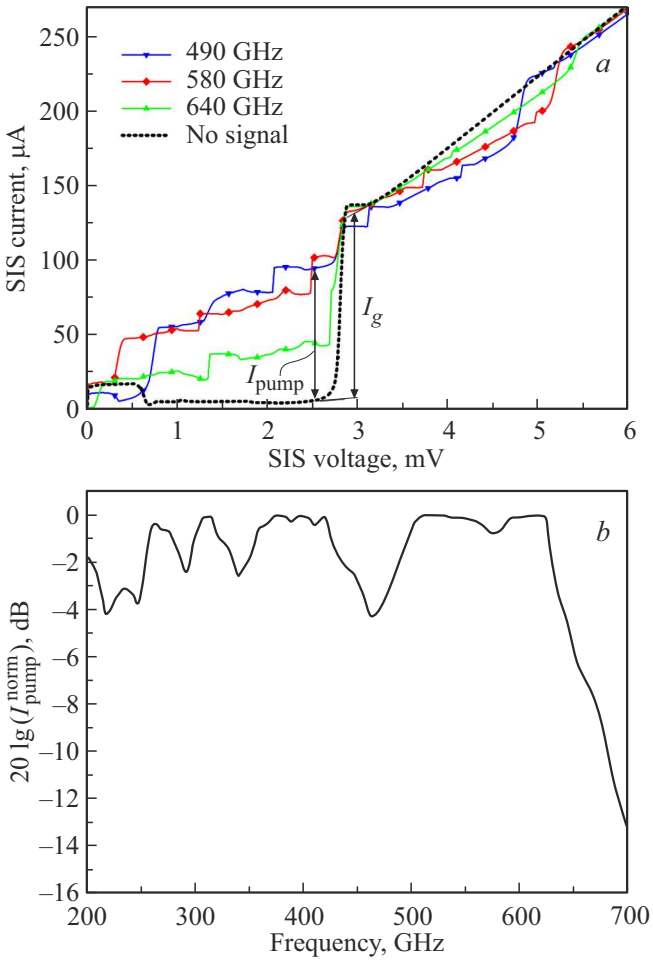

Figure 2. *a*) VAC of the SIS detector under the influence of a microwave signal of different frequencies. I_{pump} is value of the pumping current, I_g is value of the current jump across the gap. *b*) Measured dependence of the normalized detector pumping current on frequency. The detector was the SIS junction, the VAC of which is shown in Fig. 2, *a*.

It should be noted that in many cases the generator produces too much power, and at the corresponding frequencies the detector operates in saturation mode (the pumping current reaches I_g). During processing, all measurements obtained for FFO currents greater than the saturation current are not taken into account, and the matching curve reaches the maximum level (see Fig. 2, *b*).

3. Mathematic simulation of transmission lines

To optimize the integral matching structures, a model of the matching circuit was built in a mathematic simulation program. The impedance conversion that each transformer produces depends on its own impedance and length. The transformer consists of several microstrip lines, which are connected by a trapezoidal electrode. When constructing the calculation, the places of expansion and narrowing were approximated by a stepped chain of short microstrip lines. Its impedance Z_B depends on the width of the strip W, the thickness of the insulator H and its permittivity ε_{eff} as follows [14,15]:

$$Z_B = \frac{1}{\sqrt{\varepsilon_{\text{eff}}}} \frac{120\pi}{1.4 + W/H + 0.7\ln(W/H + 1.4)}.$$

The inclusion of superconductivity effects in the calculations was implemented by adding corrections to the impedance Z_B and resistance constant γ, which take into account the penetration of the magnetic field and attenuation in the line and depend on the surface impedance of the superconducting electrodes. Wave impedance Z_o^S and propagation constant γ^S in a line with superconducting electrodes can be calculated as follows:

$$Z_o^S = Z_B\sqrt{A^2 + \frac{1}{i\omega L}\left(\frac{R^t}{W^t} + \frac{R^b}{W^b}\right)},$$

$$\gamma^S = \gamma\sqrt{A^2 + \frac{1}{i\omega L}\left(\frac{R^t}{W^t} + \frac{R^b}{W^b}\right)},$$

where the Swihart's factor A is equal to

$$A = \sqrt{1 + \frac{\lambda^t}{H}\coth\left(\frac{\lambda^t}{d^t}\right) + \frac{W^t}{W^b}\frac{\lambda^b}{H}\coth\left(\frac{\lambda^b}{d^b}\right)}.$$

Here λ is London depth of penetration of the magnetic field into the superconductor, d is electrode thickness, R is surface resistance, indices t and b indicate the parameters of the upper and bottom electrodes, respectively.

The calculation is made in two ways. In the first case, the impedance matching factor is calculated between the various parts of the circuit, from the source to the detector. The result is shown in Fig. 3.

In the second method, the transfer matrices of circuit elements (ABCD matrices) [14,15] are compiled and the ratio of the power incident on the SIS junction to the power

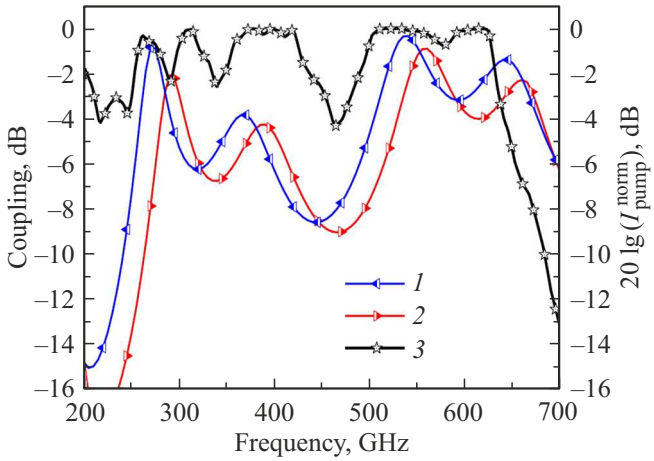

Figure 3. Frequency dependence of the normalized pumping current. Comparison of experiment with calculation results: curve *1* is impedance matching, *2* are ABCD matrices, *3* is experimental data. The values of the theoretical curves refer to the axis on the left, the value of the experimental curve refers to the axis on the right.

radiated by the generator is calculated [16]. The matrix of a microstrip line of constant width has the form [14,15]:

$$\mathbf{M} = \begin{pmatrix} \text{ch}(\gamma l) & Z_o^S \,\text{sh}(\gamma l) \\ \dfrac{1}{Z_o^S}\,\text{sh}(\gamma l) & \text{ch}(\gamma l) \end{pmatrix},$$

where l is element length. At frequencies above 700 GHz, where the radiation quantum energy becomes comparable and may even exceed the energy gap of niobium, the signal from the generator is heavily absorbed in the superconducting electrodes of the transmission line; this effect was taken into account in the second calculation method. The sheet resistance of the electrode was calculated using the formulas of the Mattis–Bardeen theory [17], which take into account the effects of strong coupling [18].

Comparison of calculations with experimental data is shown in Fig. 3. The thickness of SiO_2 in the sample is 250 nm. The detector was the SIS junction, the CVC of which is shown in Fig. 2, *a*. It is possible to note a good coincidence of peaks in frequency both between the two calculations and both calculations with the experiment. For a correct assessment and interpretation of the comparison results, it is also necessary to take into account the features directly related to the generation of radiation, since for the FFO there is a dependence of the radiation power on frequency. Thus, for Nb−AlO_x−Nb structures at generation frequencies of about 450 GHz (voltage $V_g/3$, where V_g is the gap voltage), the FFO generation mode changes: from the Fiske steps, a transition to the flux-flow mode takes place. This transition is caused by the self-pumping effect [19,20]. As a result, the power up to frequency of 450 GHz will be somewhat higher than the calculated one, and after it will be noticeably lower due to additional losses

in the FFO itself. The difference in matching levels between theoretical models at high frequencies is due to the fact that the model with ABCD matrices takes into account losses at frequencies above the gap frequency. The incomplete correspondence between the position of the peaks of the theoretical and experimental curves on the frequency axis is caused by the frequency dependence of the London penetration depth of the magnetic field. The pumping observed in the experiment at low frequencies is due to the generation of the FFO at the harmonics of the Josephson frequency [21]. In this work, it is shown that the pumping observed at frequencies 200–350 GHz is „the replica“ of pumping compressed in half along the frequency axis at frequencies of 400–700 GHz.

4. Experimental results and discussion

When comparing experimental data with the results of calculations, the main attention should be paid to the qualitative agreement of the presented curves and the position of peaks and dips in the matching curve, and not to the quantitative agreement of the pumping levels. In the calculation, the result is the power level reaching the SIS junction, and in the experiment, the pumping current is measured, which is related to the incoming power level by a rather complex dependence [13]; therefore, all diagrams presented have a double vertical axis.

The resulting mathematical models were applied to create devices operating in the range of 450–700 GHz, below are examples of the successful use of these models. Integrated circuits containing various variants of matching structures have been developed, prepared and studied. Comparison of the calculation with the experiment allows you to refine the calculation models and determine the values of the parameters that allow you to get the best matching with the experiment. Two matching schemes have been implemented, differing in the impedance transformer between the low frequency insertion element and the SIS detector; the results are shown in Fig. 4. For the first schema (Fig. 4, *a*), the transformer is traditionally a two-stage one (element *4* in the circuit in Fig. 1). In the second schema (Fig. 4, *b*), the single-stage transformer was used in front of the microstrip line containing the SIS detector, which makes it possible to shorten the length of the lines and reduce the effect of losses at high frequencies close to the gap superconductor frequency. For both variants, in most of the 450–700 GHz range, the power loss is from 4 to 1 dB. Predictably, the variant with the single-stage transformer has a lower matching bandwidth (550–620 GHz in −3 dB level compared to the range of 500–650 GHz for the two-stage transformer), but it makes it possible to reduce losses due to the shorter length of the structure, which may be important when operating at frequencies around 1 THz.

The Nb–AlO_x–Nb Josephson junction was used as a detector. Main parameters: $R_nS = 27.2\,\Omega\cdot\mu\text{m}^2$, $S = 1.24\,\mu\text{m}^2$. It should be noted that the results shown

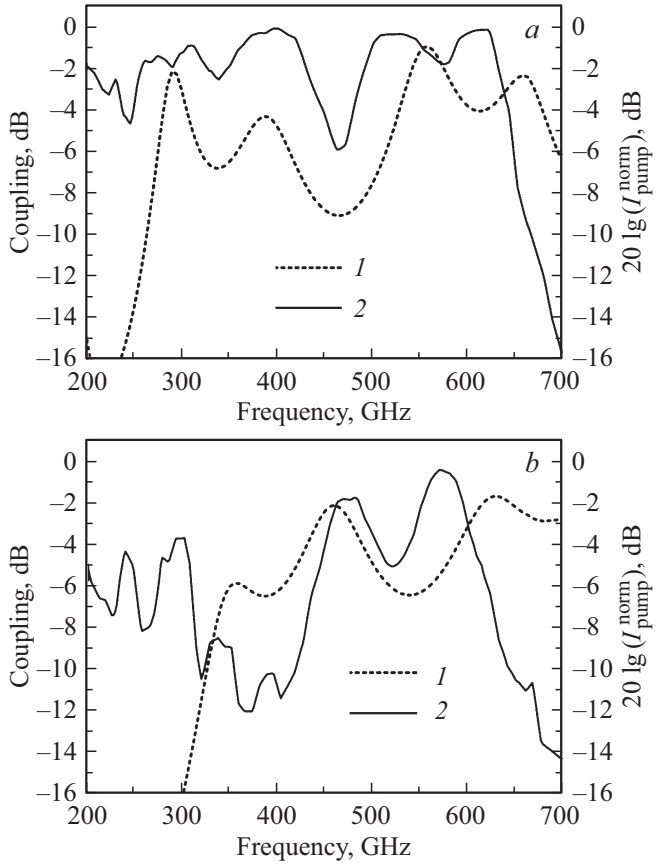

Figure 4. Frequency dependence of the normalized pumping current for *a*) two-stage and *b*) single-stage transformer in front of the detector block. Curve *1* is calculation by ABCD matrix method, *2* is experimental curve.

in Fig. 4 were obtained for samples with one SiO_2 insulator layer 250 nm thick, which simplifies the manufacturing technology. The results obtained demonstrate the possibility of implementing a fairly good matching in structures with single insulator layer: in almost the entire calculated frequency range of 450–700 GHz, the matching level lies above −4 dB.

The influence of the current density of the SIS junction on the nature of microwave signal transmission was studied. The use of receiving structures with a high tunneling current density makes it possible to significantly expand the matching band. The connection between the tunnel current in the Josephson junction and the value of the normal resistance R_n has the form

$$I = \frac{\sqrt{2\pi k_{\text{B}} T\Delta}}{eR_n}\exp\left(-\frac{\Delta}{k_{\text{B}}T}\right)\sinh\left(\frac{eV}{k_{\text{B}}T}\right),$$

where T is absolute temperature, k_{B} is Boltzmann constant, e is elementary charge, Δ is energy gap of superconductor, V is applied voltage.

It is more convenient to use an abbreviated expression that includes the value of the critical current density in the

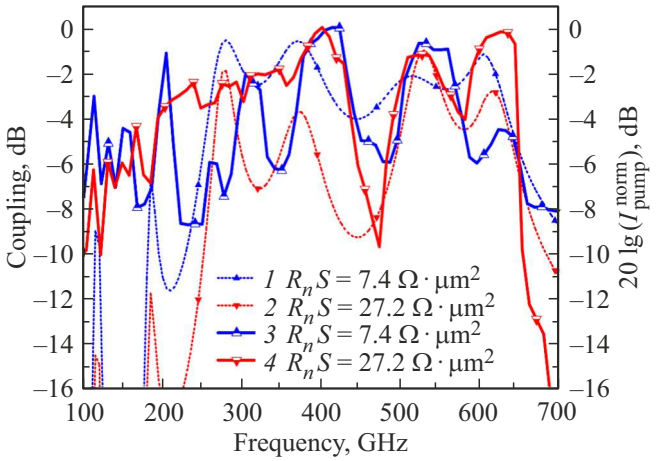

Figure 5. Frequency dependence of the normalized pumping current. Comparison of samples with identical matching structures, but different detector parameters R_nS. Curves *1, 2* is calculation by the ABCD matrix method, *3, 4* are experimental curves.

junction j_c:

$$R_nS = \frac{V_g}{j_g} = \frac{\pi}{4}\frac{V_g}{j_c}.$$

Applying it to the available samples, one can obtain the value of the tunnel current density of the SIS junction j_g in kA/cm^2:

$$j_g = \frac{\pi}{4}\frac{250}{R_nS}.$$

The impedance of the SIS detector depends on its current density. Therefore, by changing the value R_nS, and together with it the value j_g, we also change the impedance matching factor. This can be observed both in calculation and in experiment. The corresponding data are shown in Fig. 5.

Both calculations and experiment demonstrate a rather strong dependence of the signal transmission level on the current density: the lower R_nS (the higher j_g), the larger the band can effectively matching the FFO and SIS impedances. It should be noted that in order to achieve optimal matching of the receiving element with small R_nS and the external electrodynamic system, SIS junctions of submicron sizes are required.

As increase in temperature, losses in superconducting electrodes increase; this affects the quality of signal transmission through the matching structure. In addition, the mode of operation of the FFO-based generator changes substantively; due to a significant increase in the quasiparticle current, losses in the FFO itself increase, as a result of which the radiation power at high frequencies drops. As the temperature rises, the main parameters of the SIS detector also decrease: the gap voltage V_g and the value of the current jump on the gap I_g, the leakage current under the gap increases, see Fig. 6. When measuring the pumping current, all these effects were taken into account; the operating point at which the measurements took place shifted from 2.5 mV to the region of lower voltages. It can be seen from Fig. 7 that the region of effective matching shifts to the region of lower frequencies, and the matching level decreases. For comparison, the figure shows the calculated matching values for two temperatures; the calculation took into account only the change in the power transfer coefficient in the matching circuit with an increase in temperature, without taking into account the change in the FFO operating mode.

Data on the temperature dependence of the values of V_g and I_g are necessary to study the effect of temperature on the signal transfer coefficient, since the measurement of the value for current of pumping of the SIS detector cannot be adjusted without information about the gap voltage V_g, and further normalization of the obtained results is carried out with the direct participation of the I_g value.

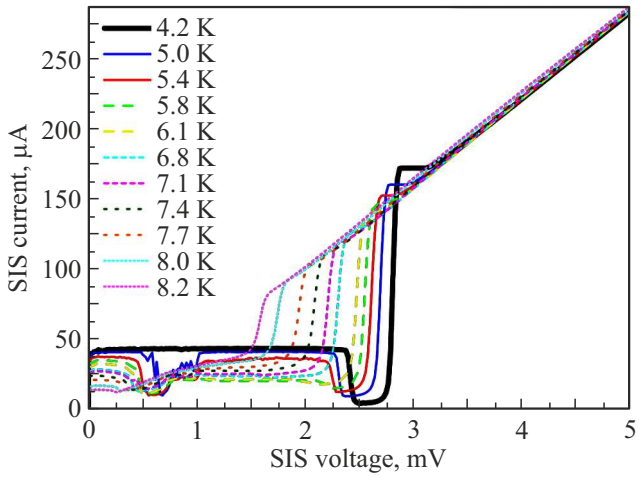

Figure 6. Volt-ampere characteristics of the SIS junction at various temperatures. The main parameters of the given SIS junction are: $R_nS = 27.2\,\Omega \cdot \mu m^2$, $S = 1.24\,\mu m^2$.

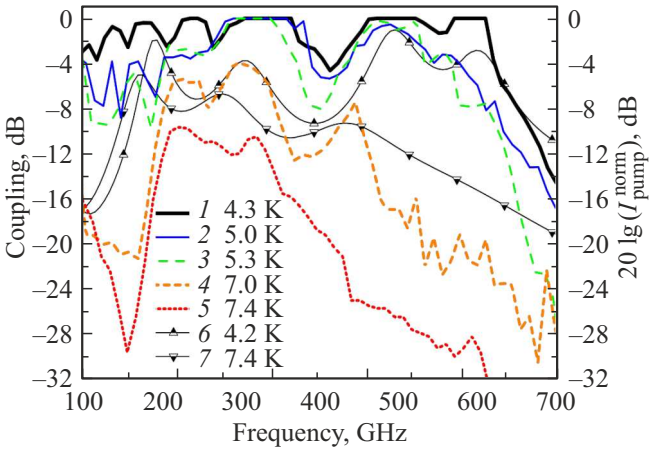

Figure 7. Dependence of calculated matching and experimental pumping current on frequency at different temperatures. Curves *1–5* are experimental curves, *6, 7* is calculation by the ABCD matrix method. The detector was an SIS junction, the VAC series of which is shown in Fig. 6.

With increase in temperature, there is a strong increase in power losses in the niobium electrodes, as well as a decrease in the FFO generation power, which was not taken into account in the calculation. It can be seen from Fig. 7 that the contribution of both effects increases with increasing frequency. The last factor, apparently, causes a noticeable difference between the calculation and the experimental results. Heating the sample to temperatures in the order of 5.0 K does not lead to a significant deterioration in signal transmission (although it entails an increase in losses at high frequencies), while a further increase in temperature actually makes the devices unusable due to the low level of signal transmission.

5. Conclusion

The results of the development, research and optimization of superconducting integrated structures designed to match the generator and the SIS detector in the frequency range of 200−750 GHz are presented. Mathematical models of integral matching structures are developed and optimized, the principles of their construction and operation are described, the influence of the main parameters of matching structures on signal transmission is determined. The modernization of the calculation algorithms made it possible to obtain a correspondence between the positions of the extrema of the calculated and experimental curves. Thanks to the developed and tested models of transmission lines, the topology of matching structures was optimized; with their help, samples were designed to operate in the 450−700 GHz frequency range. The possibility of using one-section transformers is shown, which reduces losses and makes it possible to manufacture matching structures for operation at high frequencies close to the gap frequency: on level −3 dB operating range is from 550 to 620 GHz. The studies performed have confirmed the possibility of a significant expansion of the matching band for samples with detectors based on SIS junctions with a high tunneling current density. The possibility of effective matching (above −4 dB in the calculated frequency range) for structures with a constant insulator layer thickness is demonstrated, which simplifies the manufacturing technology. It is calculated that changing the R_nS value of the detector from $7.4\,\Omega\cdot\mu\mathrm{m}^2$ to $27.2\,\Omega\cdot\mu\mathrm{m}^2$ leads to the drop in matching by a few dB (−5 dB at frequency 450 GHz). The effect of temperature on the operating range of integral matching structures has been studied; it has been shown that high-quality signal transmission is possible at temperatures not exceeding 5 K.

Funding

The study was performed with the support of the Russian Science Foundation grant No. 20-42-04415. The preparation of the experimental structures was carried out within the framework of the State Assignment of Kotelnikov Institute of Radio Engineering and Electronics of RAS. For the studies, the equipment of Unique Scientific Facility No. 352529 „Cryointegral“ was used, the development of which was supported by the grant from the Ministry of Science and Higher Education of the Russian Federation, agreement No. 075-15-2021-667.

Conflict of interest

The authors declare that they have no conflict of interest.

References

[1] V.P. Koshelets, S.V. Shitov. Supercond. Sci. Technol. **13**, *5*, R53 (2000). DOI:710.1088/0953-2048/13/5/201
[2] V.P. Koshelets, P.N. Dmitriev, M.I. Faley, L.V. Filippenko, K.V. Kalashnikov, N.V. Kinev, O.S. Kiselev, A.A. Artanov, K.I. Rudakov, A. de Lange, G. de Lange, V.L. Vaks, M.Y. Li, H.B. Wang. IEEE Trans. Terahertz Sci. Technol. **5**, *4*, 687 (2015). DOI: 10.1109/TTHZ.2015.2443500
[3] M.S. Shevchenko, A.A. Atepalikhin, F.V. Khan, L.V. Filippenko, A.M. Chekushkin, V.P. Koshelets. IEEE Trans. Appl. Supercond. **32**, *4*, 1100205 (2022). DOI: 10.1109/TASC.2021.3130103
[4] T. Nagatsuma, K. Enpuku, F. Irie, K. Yoshida. J. Appl. Phys. **54**, *9*, 3302 (1983). DOI: 10.1063/1.332443
[5] T. Nagatsuma, K. Enpuku, F. Irie, K. Yoshida. J. Appl. Phys. **56**, *11*, 3284 (1984). DOI: 10.1063/1.333849
[6] V.P. Koshelets, P.N. Dmitriev, A.S. Sobolev, A.L. Pankratov, V.V. Khodos, V.L. Vaks, A.M. Baryshev, P.R. Wesselius, L. Mygind. Physica C **372**, *Part I*, 316 (2002). DOI: 10.1016/S0921-4534(02)00659-7
[7] P.N. Dmitriev, L.V. Filippenko, V.P. Koshelets. In: Josephson Junctions. History, Devices, and Applications / Eds E. Wolf, G. Arnold, M. Gurvitch, J. Zasadzinski. Pan Stanford Publishing Pte. Ltd. (2017). Ch. 7. P. 185−244. ISBN 978-981-4745-47-5 (hard cover), ISBN 978-1-315-36452-0 (eBook)
[8] P.N. Dmitriev, A.B. Ermakov, N.V. Kinev, O.S. Kiselev, L.V. Filippenko, M.Y. Fominskii, V.P. Koshelets. J. Commun. Technol. Electron. **66**, *4*, 473 (2021). DOI: 10.1134/S1064226921040033
[9] L.V. Filippenko, S. Shitov, P.N. Dmitriev, A.B. Ermakov, V.P. Koshelets, J.-R. Gao. IEEE Trans. Appl. Supercond. **11**, *1*, 816 (2001). https://doi.org/10.1109/77.919469
[10] M.Y. Torgashin, V.P. Koshelets, P.N. Dmitriev, A.B. Ermakov, L.V. Filippenko, P.A. Yagoubov. IEEE Trans. Appl. Supercond. **17**, *2*, 379 (2007). https://doi.org/10.1109/tasc.2007.898624
[11] G. De Lange, M. Birk, D. Boersma, J. Dercksen, P. Dmitriev, A.B. Ermakov, L.V. Filippenko, H. Golstein, R.W.M. Hoogeveen, L. De Jong, A.V. Khudchenko, N.V. Kinev, O.S. Kiselev, B. van Kuik, A. de Lange, J. van Rantwijk, A.M. Selig, A.S. Sobolev, M.Yu. Torgashin, E. de Vries, G. Wagner, P.A. Yagoubov, V.P. Koshelets. Supercond. Sci. Technol. **23**, *4*, 045016 (2010). https://doi.org/10.1088/0953-2048/23/4/045016
[12] K.I. Rudakov, A.V. Khudchenko, L.V. Filippenko, M.E. Paramonov, R. Hesper, D.A.R. da Costa Lima, A.M. Baryshev, V.P. Koshelets. Appl. Sci. **11**, *21*, 10087 (2021). DOI: 10.3390/app112110087
[13] J.R. Tucker, M.J. Feldman. Rev. Mod. Phys. **57**, *4*, 1055 (1985). DOI: 10.1103/RevModPhys.57.1055

[14] V.F. Fusco. Microwave circuits: analysis and computer-aided design. Prentice Hall (1987).
[15] S.I. Bakharev, V.I. Volman, Yu.N. Lib, N.M. Mamonova, A.D. Muravtsov, A.G. Sarkisyants, R.A. Silin, O.K. Slavinsky, D.D. Shiryaev. Spravochnik po raschetu i konstruirovaniyu SVCh poloskovykh ustroystv. Radio i svyaz, M. (1982). 325 p. (in Russian).
[16] D.A. Frickey. Microwave. Opt. Technol. Lett. **5**, *12*, 613 (1992). DOI: 10.1002/mop.4650051203
[17] D.C. Mattis, J. Bardeen. Phys. Rev. **111**, *2*, 412 (1958). DOI: 10.1103/PhysRev.111.412
[18] T. Noguchi, T. Suzuki, T. Tamura. IEEE Trans. Appl. Supercond. **21**, *3*, 756 (2011). DOI: 10.1109/TASC.2010.2089033
[19] V.P. Koshelets, S.V. Shitov, A.V. Shchukin, L.V. Filippenko, J. Mygind, A.V. Ustinov. Phys. Rev. B **56**, *9*, 5572 (1997). DOI: 10.1103/PhysRevB.56.5572
[20] D.R. Gulevich, V.P. Koshelets, F.V. Kusmartsev. Phys. Rev. B **96**, *2*, 024515 (2017). https://doi.org/10.1103/PhysRevB.96.024515
[21] N.V. Kinev, K.I. Rudakov, L.V. Filippenko, V.P. Koshelets. IEEE Trans. Appl. Supercond. **32**, *4*, 1500206 (2022). DOI: 10.1109/TASC.2022.3143483